

RESEARCH

Open Access



Deciphering the role of SAMHD1 in endometrial cancer progression

Ping Qiang¹, Ying Chen², Yang Shao¹, Qicheng Deng², Songyuan Xu¹ and Weipei Zhu^{2*}

Abstract

Background Endometrial cancer (EC) presents significant clinical challenges due to its heterogeneity and complex pathophysiology. SAMHD1, known for its role as a deoxynucleotide triphosphate triphosphohydrolase, has been implicated in the progression of various cancers, including EC. This study focuses on elucidating the role of SAMHD1 in EC through its impact on TRIM27-mediated PTEN ubiquitination.

Results Utilizing a combination of bioinformatics and cellular biology techniques, we investigated the interactions among SAMHD1, TRIM27, and PTEN. Our findings reveal that SAMHD1 modulates PTEN ubiquitination via TRIM27, impacting key pathways involved in EC pathogenesis. These interactions suggest a critical mechanism by which SAMHD1 could influence tumor behavior and progression in EC.

Conclusions The results from this study underscore the potential of targeting the SAMHD1-TRIM27-PTEN axis as a therapeutic strategy in EC. By providing new insights into the molecular mechanisms underlying EC progression, our research supports the development of novel therapeutic approaches that could contribute to improve treatment strategies for patients with EC.

Keywords dNTP hydrolysis enzyme, SAMHD1, TRIM27, Ubiquitination, PTEN, PI3K/AKT signaling pathway

Background

Endometrial cancer (EC) is one of the most common gynecological malignancies worldwide, with its incidence steadily increasing, posing a significant threat to women's health [1]. Similar to many other cancers, the occurrence and progression of EC result from the combined effects of multiple genes, cellular pathways, and factors [2, 3]. Patients with EC have various treatment options

to choose from, some of which are standard therapies (currently commonly used treatments), while others are in clinical trial phases. The standard treatments currently utilized include surgery, radiation therapy, chemotherapy, hormone therapy, and biological therapy [4–7]. Although significant progress has been made in the prevention, diagnosis, and treatment of EC, the treatment outcomes are still not satisfactory due to its complex molecular mechanisms and various molecular subtypes [8]. Therefore, it is crucial to conduct in-depth research on the pathogenesis of EC and key molecular regulatory networks. This research can provide new biomarkers for early diagnosis and prognostic assessment of EC, as well as potentially pave the way for targeted therapies [9].

In recent years, researchers have been increasingly focusing on the role of molecules and proteins associated with cancer. SAMHD1 has undoubtedly become a

*Correspondence:

Weipei Zhu
zwp3333@suda.edu.cn

¹Department of Obstetrics and Gynecology, The First People's Hospital of Zhangjiagang City, The Zhangjiagang Affiliated Hospital of Soochow University, Suzhou 215600, China

²Department of Obstetrics and Gynecology, The Second Affiliated Hospital of Soochow University, No. 1055, Sanxiang Road, Suzhou, Jiangsu Province 215000, China



© The Author(s) 2024. **Open Access** This article is licensed under a Creative Commons Attribution-NonCommercial-NoDerivatives 4.0 International License, which permits any non-commercial use, sharing, distribution and reproduction in any medium or format, as long as you give appropriate credit to the original author(s) and the source, provide a link to the Creative Commons licence, and indicate if you modified the licensed material. You do not have permission under this licence to share adapted material derived from this article or parts of it. The images or other third party material in this article are included in the article's Creative Commons licence, unless indicated otherwise in a credit line to the material. If material is not included in the article's Creative Commons licence and your intended use is not permitted by statutory regulation or exceeds the permitted use, you will need to obtain permission directly from the copyright holder. To view a copy of this licence, visit <http://creativecommons.org/licenses/by-nc-nd/4.0/>.

hot research subject [10–12]. SAMHD1, short for sterile alpha motif domain and histidine/aspartate-rich domain-containing protein 1, is a dNTP hydrolase involved in various biological processes, including DNA damage repair, cell cycle regulation, and immune response [13, 14]. Recent studies have found that SAMHD1 undergoes significant changes in expression and function in various types of cancer, suggesting that it may play a key role in the onset and progression of cancer [10].

In addition to the well-known functions of SAMHD1, TRIM27 and PTEN are also crucial molecules in cancer research [15, 16]. TRIM27, an E3 ubiquitin ligase, plays a key role in the ubiquitination process that regulates protein stability and activity, thereby impacting various cellular processes [17]. Previous studies have suggested that TRIM27 promotes the PI3K/AKT signaling pathway by interacting with phosphatases and reducing PTEN activity [15, 18]. PTEN is a critical tumor suppressor, and its inactivation or mutation is frequently linked to the development and progression of multiple cancer types, including endometrial, prostate, and lung cancers [2, 3, 19]. Consequently, it is hypothesized that SAMHD1 may influence cancer progression by modulating TRIM27-mediated ubiquitination of PTEN, affecting cancer cell proliferation, migration, and invasion.

Against this backdrop, our study aims to thoroughly investigate the impact of SAMHD1-regulated TRIM27-mediated PTEN ubiquitination on the occurrence and progression of EC. Leveraging state-of-the-art bioinformatics techniques and cell biology methods, we seek to elucidate the relationships between SAMHD1, TRIM27, and PTEN, and their roles in EC. Through this research, we have uncovered the association between SAMHD1-regulated TRIM27-mediated PTEN ubiquitination and EC, paving the way for novel targeted strategies for EC treatment to enhance therapeutic outcomes and patients' quality of life, which carries significant scientific and clinical implications. Furthermore, we have delved into the key molecular regulatory networks underlying the pathogenesis of EC, potentially providing new biomarkers for early diagnosis and prognosis assessment of EC, as well as opening avenues for targeted EC therapies.

Results

SAMHD1 promotes the proliferation, migration, and invasion of EC cells

Previous studies have shown that SAMHD1 is oncogenic in leukemia, breast, ovarian, and non-small cell lung cancer [20, 21]. A study by An et al. [22] has reported that SAMHD1 can induce intracellular FAK signaling to promote the migration of human renal clear cell carcinoma through the activation of Rac1-mediated lamellipodia formation. Additionally, SAMHD1 is highly expressed in various cancer cells. However, the precise mechanism

of SAMHD1 in EC remains unclear. We analyzed the ENCORI database and found that SAMHD1 expression levels are higher in EC samples from TCGA. Additionally, based on datasets from GSE17025 and GSE63678, we also found higher expression of SAMHD1 in EC (Fig. 1A).

In this study, we detected the expression of SAMHD1 in EC cell lines. The results showed that the expression of SAMHD1 was higher in four EC cell lines (KLE, HEC-1-B, RL95-2, Ishikawa) compared to the normal immortalized endometrial stromal cell line SHT290. Among them, SAMHD1 expression was higher in the HEC-1-B cell lines and lower in the Ishikawa, KLE and RL95-2 cell lines (Fig. 1B). Therefore, we chose the Ishikawa cell line for overexpression of the SAMHD1 gene and the HEC-1-B cell line for silencing the SAMHD1 gene. The overexpression efficiency of oe-SAMHD1 in the Ishikawa cell line was confirmed by qRT-PCR and Western blot (Fig. 1C-D). Cell proliferation was detected by CCK8 assay, and it was found that overexpression of SAMHD1 promoted the proliferation of EC cells (Fig. 1E).

Similarly, qRT-PCR and Western blot validated the efficiency of silencing the SAMHD1 gene in HEC-1-B cells using different shRNA sequences. Due to the high knockout efficiency of shRNA#2, we ultimately selected shRNA#2 as the experimental object (Fig. 1F-G). Validation of sh-SAMHD1-2 and sh-SAMHD1-3 was performed using the CCK-8 method. The results indicate that sh-SAMHD1-3 has a minor effect on cell proliferation, while sh-SAMHD1-2 significantly influences cell proliferation. It was observed that silencing SAMHD1 can inhibit the proliferation of EC cells (Fig. 1H). Cell migration was assessed using a scratch assay, and it was found that overexpression of SAMHD1 promoted the migration and invasion of EC cells Ishikawa (Fig. 1I-J). Western blot results showed a significant increase in the expression of N-cad, Vim, Twist, and Snail, while E-cad expression was reduced (Fig. 1K). Silencing SAMHD1 inhibited HEC-1-B and KLE EC cell migration and invasion (Fig. 1L-M). Western blot results showed a significant decrease in the expression of N-cad, Vim, Twist, and Snail, while E-cad expression increased after silencing SAMHD1 (Fig. 1N). To further validate the role of SAMHD1, we selected the SAMHD1 inhibitor TH6342 to assess the migration, invasion, and expression of associated proteins in HEC-1-B cells. The results demonstrate a marked inhibition of migration and invasion in HEC-1-B cells upon treatment with TH6342 (Fig. 1O). Moreover, the expression levels of N-cadherin, Vimentin, Twist, and Snail were significantly reduced, while E-cadherin expression was enhanced in the TH6342 inhibitor-treated group (Fig. 1P). These findings align with the outcomes of SAMHD1 silencing.

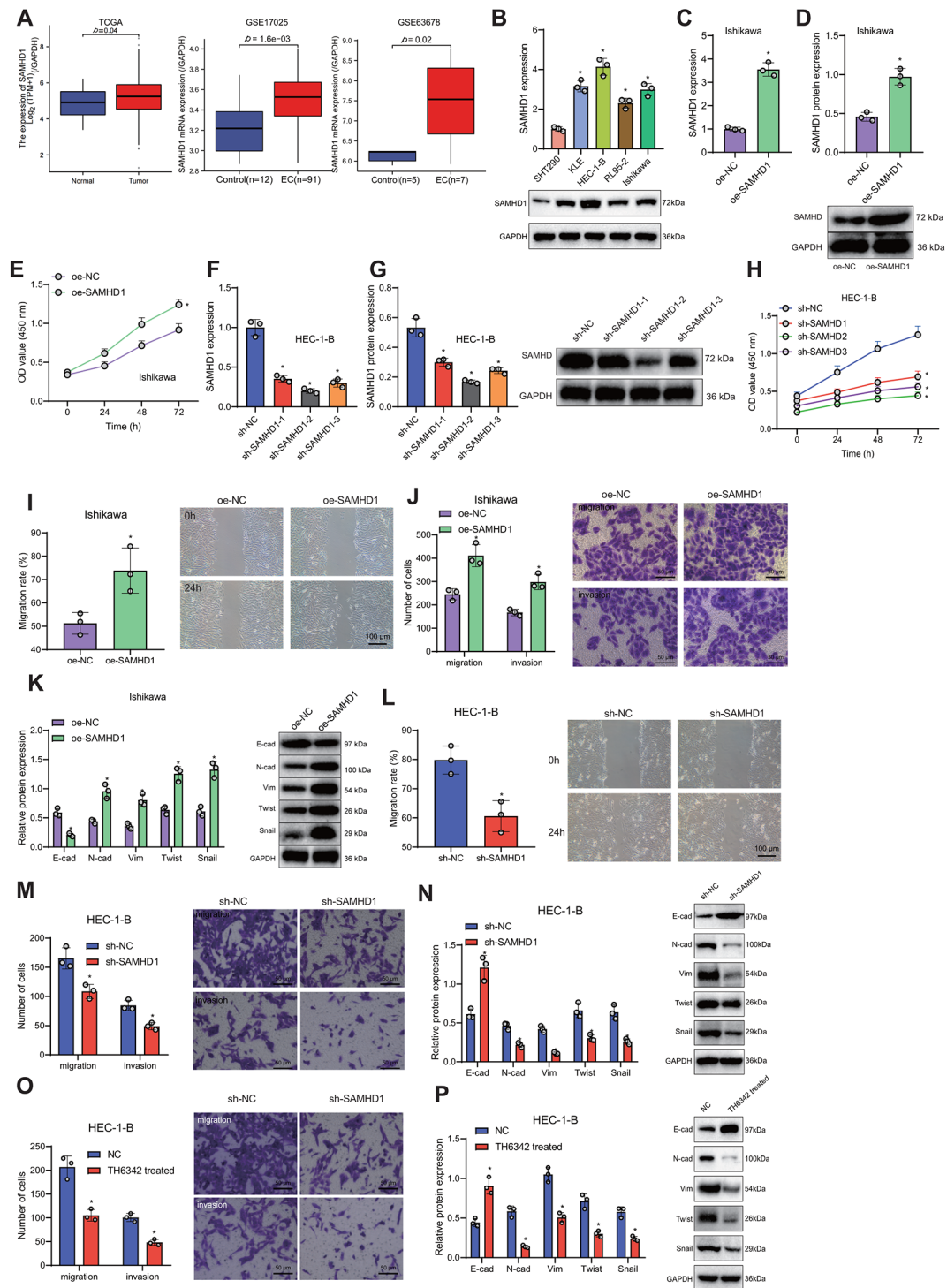


Fig. 1 (See legend on next page.)

SAMHD1 promotes EC cell tumorigenesis in nude mice

To investigate the effect of SAMHD1 on the *in vivo* growth of EC cells, we stably overexpressed SAMHD1 (oe-SAMHD1) in Ishikawa cells and stably silenced SAMHD1 (sh-SAMHD1) in HEC-1-B cells, along with corresponding control groups (oe-NC and sh-NC). These

cells were then implanted into nude mice for subcutaneous tumor formation experiments. Analysis of tumor size and weight in each group revealed that compared to the oe-NC group, the tumor volume and weight were significantly increased in the oe-SAMHD1 group. On the other hand, compared to the sh-NC group, the tumor

(See figure on previous page.)

Fig. 1 The effects of overexpression or silence of SAMHD1 on the proliferation, migration, and invasion abilities of endometrial cancer cells. **Note (A)** In the TCGA, GSE17025, and GSE63678 datasets, the expression of SAMHD1 in endometrial cancer samples, ovarian cancer, and SAMHD1 expression in cancer-adjacent samples was examined. The TCGA and GSE17025 data were both normalized using TPM, while the GSE63678 data was normalized using FPKM; **(B)** Western blot detection of SAMHD1 expression in different endometrial cancer cell lines; **(C)** qRT-PCR detection of the efficiency of SAMHD1 overexpression; **(D)** Western blot detection of SAMHD1 expression in stable SAMHD1 overexpressing endometrial cancer cell lines; **(E)** CCK8 assay to assess the proliferation capacity of SAMHD1 overexpressing cell lines; **(F)** qRT-PCR detection of the efficiency of SAMHD1 knockdown; **(G)** Western blot detection of SAMHD1 expression in stable SAMHD1 knockdown endometrial cancer cell lines; **(H)** CCK8 assay to assess the proliferation capacity of SAMHD1 knockdown cells; **(I)** Scratch assay to assess the migration ability of Ishikawa cell line overexpressing SAMHD1; **(J)** Transwell assay to assess the invasion ability of Ishikawa cell line overexpressing SAMHD1; **(K)** Western blot detection of EMT-related proteins; **(L)** Scratch assay to assess the migration ability of SAMHD1 knockdown cells; **(M)** Transwell assay to assess the invasion ability of SAMHD1 knockdown cells (50 μ m); **(N)** Western blot detection of EMT-related proteins; **(O)** Migration and invasion assay of HEC-1-B cells treated with SAMHD1 inhibitor TH6342; **(P)** Western blot analysis of EMT-related proteins (N-cadherin, Vimentin, Twist, Snail, E-cadherin) in TH6342-treated HEC-1-B cells. (The statistical analysis employed mean \pm standard deviation representation. For comparing two groups, an independent samples t-test was used, while one-way ANOVA was utilized for comparing three or more groups. Data from different time points were analyzed using two-way ANOVA. ** indicates statistical significance compared to the oe-NC or sh-NC group, where $P < 0.05$ signifies a significant difference. The experiments were repeated three times.)

volume and weight were significantly decreased in the sh-SAMHD1 group (Fig. 2A-B). qRT-PCR analysis of SAMHD1 mRNA expression in the subcutaneous tumor tissues showed that compared to the oe-NC group, SAMHD1 mRNA expression was significantly increased in the oe-SAMHD1 group.

Similarly, compared to the sh-NC group, SAMHD1 mRNA expression was significantly decreased in the sh-SAMHD1 group (Fig. 2C). Results from H&E staining showed increased tumor tissue formation and denser morphology in the SAMHD1 overexpression group while silencing SAMHD1 resulted in decreased tumor tissue formation (Fig. 2D). TUNEL analysis of cell apoptosis demonstrated that compared to the oe-NC group, tumor cell apoptosis was reduced in the oe-SAMHD1 group. In contrast, compared to the sh-NC group, tumor cell apoptosis was increased in the sh-SAMHD1 group (Fig. 2E). Immunohistochemical staining with Ki67 showed a significantly increased proliferation rate of tumor cells in the oe-SAMHD1 group compared to the oe-NC group. Additionally, the sh-SAMHD1 group exhibited a significantly decreased proliferation rate of tumor cells compared to the sh-NC group (Fig. 2F).

SAMHD1 plays a role in promoting the occurrence and development of EC through the activation of the PI3K/AKT signaling pathway

Due to the fact that EC mostly originates from epithelial cells and the epithelial-mesenchymal transition (EMT) process plays a crucial role in the migration and invasion of epithelial-derived tumors [23, 24], we conducted qRT-PCR and Western blot analysis of EMT-related molecules in Ishikawa cells. The results revealed that overexpression of SAMHD1 decreased the expression of E-cadherin (E-cad) and increased the expression of N-cadherin (N-cad), vimentin (Vim), Twist, and the zinc finger transcription factor Snail (Fig. 3A-B). Conversely, silencing SAMHD1 in HEC-1-B cells produced opposite results (Fig. S1A-B), suggesting that SAMHD1 promotes cancer progression through the EMT process.

To further investigate the specific molecular mechanisms by which SAMHD1 regulates the EMT process, we selected the PI3K and AKT signaling pathways, which are associated with the migration and invasion of EC, based on a literature review [25, 26], and examined the molecules related to these pathways. The results showed that in Ishikawa cells overexpressing SAMHD1, the expression of phosphorylated PI3K and AKT increased (Fig. 3C), while in HEC-1-B cells with silenced SAMHD1, the expression of phosphorylated PI3K and AKT decreased (Fig. S1C).

To demonstrate that SAMHD1 mediates EC occurrence and progression through the PI3K/AKT signaling, we treated HEC-1-B cells with 740 Y-P (PI3K activator) and SC-79 (AKT activator) on the basis of silenced SAMHD1. Western blot analysis revealed that upon PI3K/AKT activation, the phosphorylation of PI3K and AKT increased, restoring the decreased expression of N-cad, Vim, Twist, and Snail, and enhancing E-cad expression induced by SAMHD1 silencing (Fig. 4A). Moreover, PI3K/AKT activation could reverse the inhibition of EC cell proliferation, migration, and invasion caused by silenced SAMHD1 (Fig. 4B-D). In conclusion, our findings indicate that silencing SAMHD1 affects EC development by inhibiting the activation of the PI3K-AKT signaling pathway, which can be replaced by PI3K-AKT activators.

SAMHD1 activates the PI3K/AKT signaling pathway by inhibiting PTEN activity

To delve into the underlying mechanisms through which SAMHD1 regulates the activation of the PI3K/AKT pathway, we conducted a literature review and found an association between SAMHD1 and PTEN in THP-1 cells [27]. PTEN, a critical regulator of the PI3K/AKT pathway, inhibits the conversion of PIP2 to PIP3 [16, 28]. Therefore, we investigated the relationship between SAMHD1 and PTEN. Western blot analysis revealed a significant increase in the expression levels of SAMHD1 and PTEN in the oe-SAMHD1 group compared to the

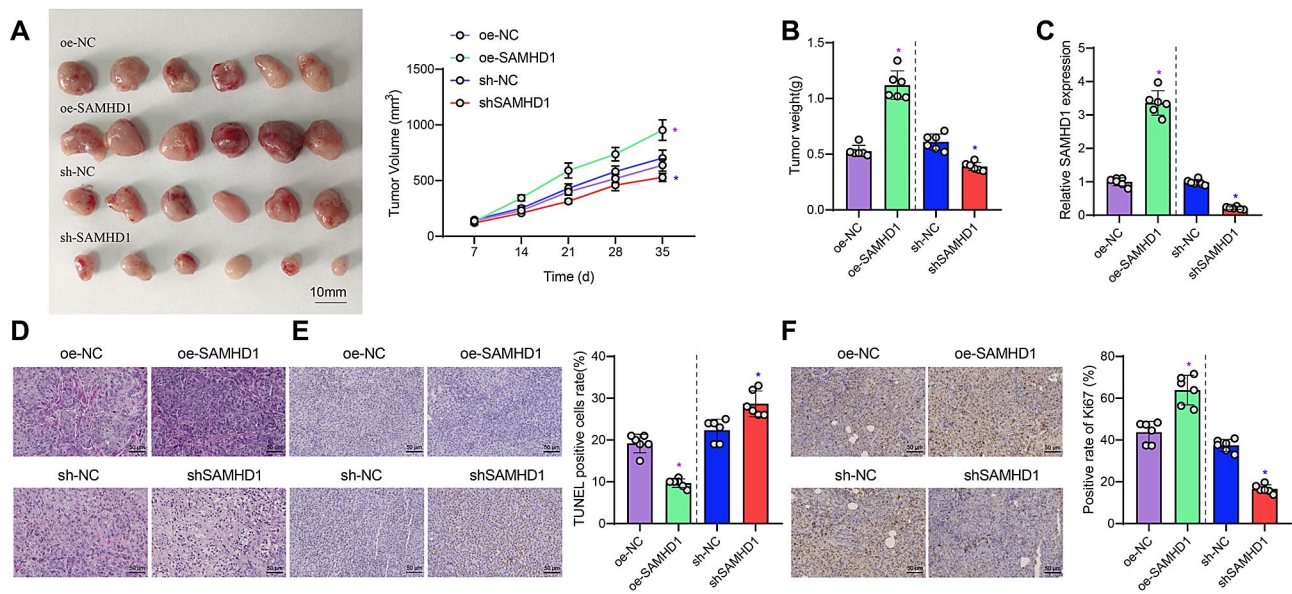


Fig. 2 The effect of overexpression or silencing of SAMHD1 on the tumor growth of endometrial cancer cells in nude mice *Note (A)* Morphology and volume of subcutaneously transplanted tumors in each group were observed; *(B)* The weight of subcutaneously transplanted tumors in each group was measured; *(C)* Expression of SAMHD1 in subcutaneously transplanted tumors of each group was detected by qRT-PCR; *(D)* Morphology of subcutaneously transplanted tumors in each group was assessed by H&E staining; *(E)* The rate of cell apoptosis in subcutaneously transplanted tumors of each group was determined by TUNEL staining; *(F)* Expression of Ki67 protein in subcutaneously transplanted tumors of each group was detected by Ki67 staining (50 μm). Purple * indicates a significant difference compared to the oe-NC group ($p < 0.05$), blue * indicates a significant difference compared to the sh-NC group ($p < 0.05$) (the data are presented as mean ± standard deviation. Group comparisons were conducted using one-way analysis of variance, while repeated measures analysis of variance was employed for comparisons across different time points)

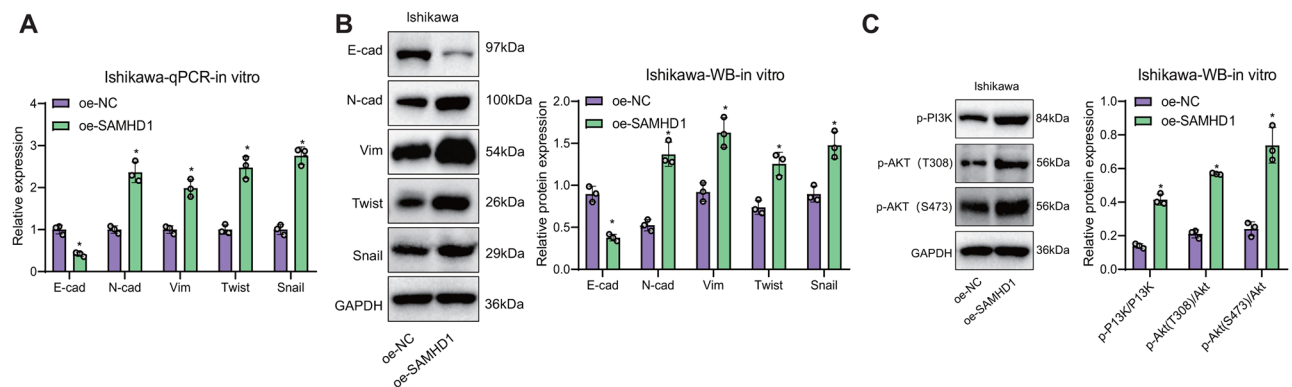


Fig. 3 Regulation of the PI3K/AKT signaling pathway in Ishikawa cells by SAMHD1. *(A)* *Note (A)* Expression analysis of EMT-related molecules post SAMHD1 overexpression using qRT-PCR; *(B)* EMT-related molecule expression analysis post SAMHD1 overexpression using Western blot; *(C)* Changes in signaling pathways like PI3K, AKT, etc., post SAMHD1 overexpression at the cellular level analyzed through Western blot; data presented as mean ± standard deviation, with analysis conducted using independent sample t-test and cell experiments repeated 3 times). * denotes significance at $p < 0.05$ compared to the oe-NC group

oe-NC group, while a marked decrease in the expression levels of SAMHD1 and PTEN was observed in the sh-SAMHD1 group (Fig. 5A). Furthermore, immunoprecipitation experiments demonstrated the interaction between SAMHD1 and PTEN, showing an increase in PTEN levels when SAMHD1 was immunoprecipitated (Fig. 5B).

To investigate the potential regulatory role of SAMHD1 in modulating the PTEN-mediated PI3K/AKT signaling

pathway, our experiments involving overexpression of SAMHD1 revealed that co-overexpression of PTEN exhibited inhibitory effects on the phosphorylation of PIP2, thereby suppressing its conversion to PIP3. This subsequently led to the enhanced phosphorylation of PI3K and AKT (p-PI3K, p-Akt) (Fig. 5C).

The protein-protein interaction between SAMHD1 and PTEN leads to the activation of the PI3K/AKT signaling pathway, indicating that SAMHD1 can indirectly

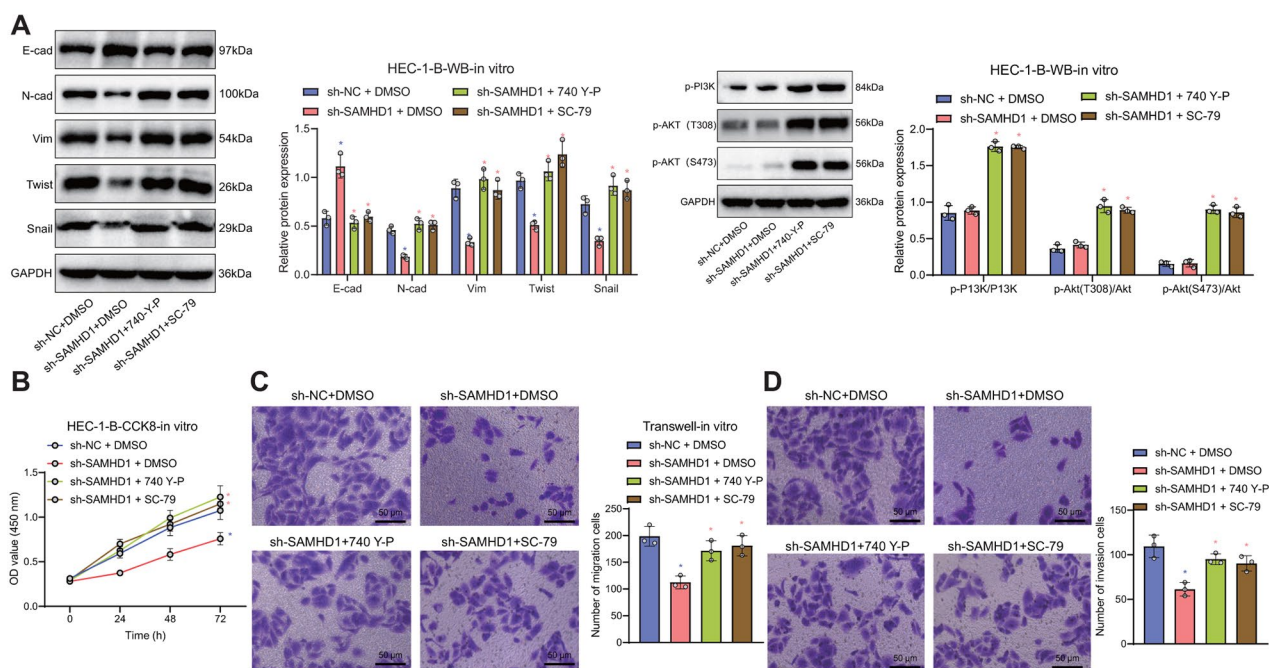


Fig. 4 SAMHD1 Regulation of the PI3K/AKT Signaling Pathway in the HEC-1-B Cells and Its Impact on Proliferation, Migration, and Invasion of Endometrial Cancer Cells. *Note* (A) Western blot analysis of the expression of EMT-related molecules in HEC-1-B cells after treatment with 740 Y-P or SC-79; (B) CCK-8 assay to evaluate the proliferation rate in SAMHD1-silenced HEC-1-B cells upon treatment with 740 Y-P/SC-79. (C-D) Transwell assay to assess the migration and invasion capabilities (50 μ m) of SAMHD1-silenced HEC-1-B cells treated with 740 Y-P/SC-79. Multiple comparisons were analyzed using one-way ANOVA. (These data are represented as quantitative data, using mean \pm standard deviation. Group comparisons were conducted using one-way analysis of variance, while different time points were analyzed using two-way analysis of variance. Blue * indicates significance compared to the sh-NC + DMSO group ($p < 0.05$), whereas pink * indicates significance compared to the sh-SAMHD1 + DMSO group ($p < 0.05$). Cell experiments were repeated three times

regulate the activation of the PI3K/AKT signaling pathway through PTEN.

SAMHD1 inhibits PTEN phosphatase activity by regulating PTEN ubiquitination mediated by TRIM27

Next, we want to investigate the specific mechanism by which SAMHD1 regulates PTEN. Ubiquitination is one of the most important ways to regulate PTEN activity, and there are already many studies suggesting that PTEN is subjected to ubiquitination modification, which affects its expression and function [29–31]. Therefore, we speculate that SAMHD1 may indirectly affect the ubiquitination process of PTEN.

The ubiquitination levels of PTEN were assessed in the normal immortalized endometrial stromal cell line SHT290 and the EC cell line HEC-1-B. The results indicated a significant reduction in PTEN ubiquitination levels in the EC cell line HEC-1-B compared to the normal immortalized endometrial stromal cell line SHT290 (Fig. 6A).

By examining the effect of SAMHD1 on the ubiquitination of PTEN in HEC-1-B cells, it was found that SAMHD1 significantly enhanced the ubiquitination modification of PTEN (Fig. 6B). Further investigation into the types of ubiquitin modifications on PTEN influenced by SAMHD1 revealed that the most common

ubiquitin modifications were K48-link (Ub-k48) and K63-link (Ub-k63), which respectively participate in protein degradation and protein stability regulation processes [32–34]. However, our experimental results showed that SAMHD1 does not affect the Ub-k48 and Ub-k63 ubiquitination modifications of PTEN. This result suggests that SAMHD1 does not regulate the function of PTEN by mediating its degradation or inhibiting its protein stability (Fig. 6C).

TRIM27 has been reported to regulate the phosphatase activity of PTEN through K27-link (Ub-k27) ubiquitination, and the phosphatase activity of PTEN is an important factor in regulating PI3K/AKT [18]. When analyzing the ENCORI database, it was found that TRIM27 is highly expressed in TCGA EC (Fig. 6D). So, does SAMHD1 participate in PTEN's Ub-k27 ubiquitination? Our experimental results showed that SAMHD1 can enhance the Ub-k27 ubiquitination of PTEN (Fig. 6E).

To further investigate how SAMHD1 regulates the Ub-k27 ubiquitination modification of PTEN, we explored the relationship between SAMHD1 and TRIM27. Analysis through the ENCORI database revealed a weak positive correlation in the expression of SAMHD1 and TRIM27 in TCGA EC samples (Fig. 6-F). Subsequently, we experimentally validated

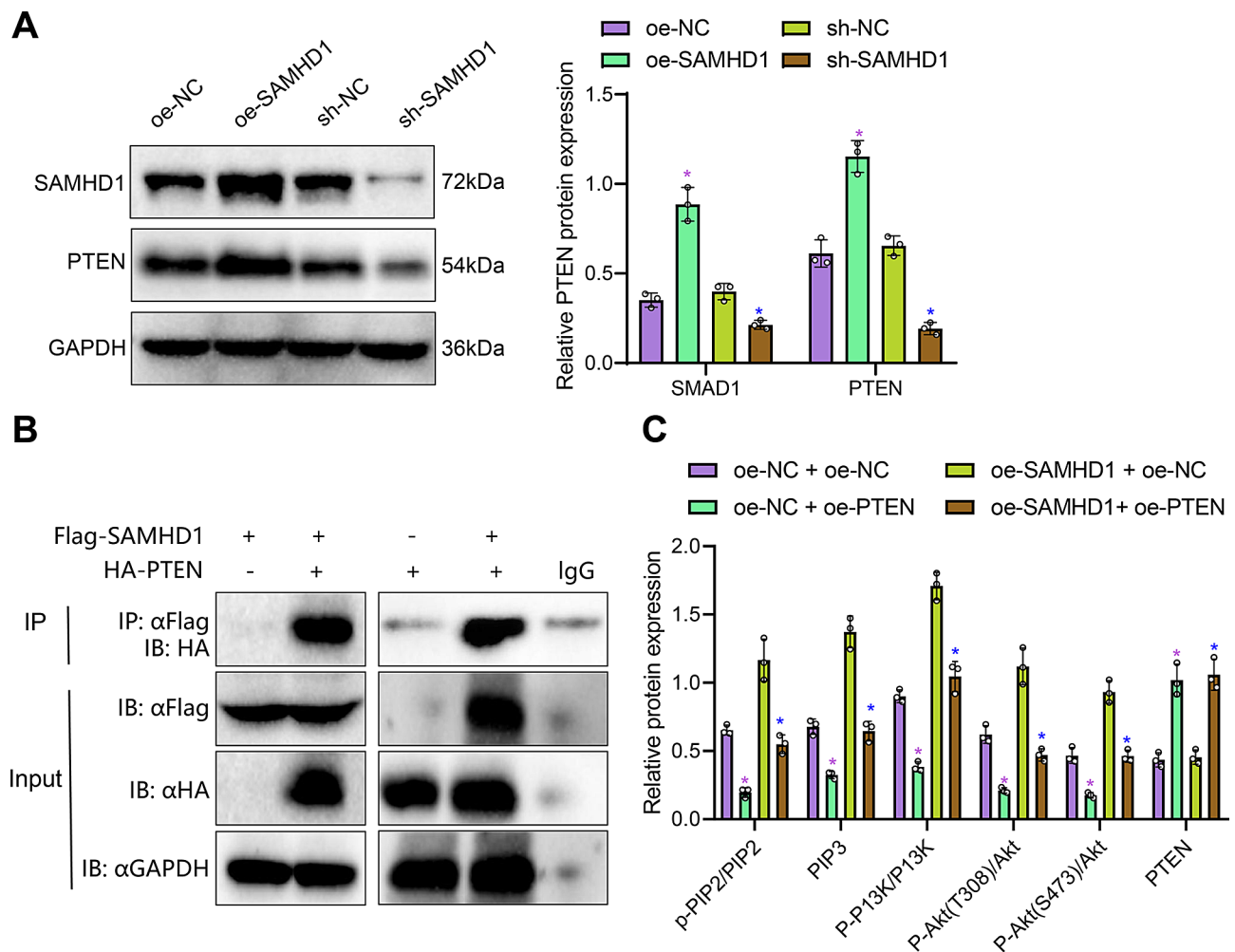


Fig. 5 SAMHD1 regulates PTEN activity to influence the activation of the PI3K/AKT signaling pathway. Note (A) Western blot detection of the effect of overexpressed SAMHD1 on PTEN expression; (B) IP to detect the interaction between SAMHD1 and PTEN; (C) Western blot detection of the inhibitory effect of overexpressed SAMHD1 on the PI3K/AKT signaling pathway of PTEN. Purple * indicates a significant difference compared to the oe-NC group or sh-NC + oe-NC group, with $p < 0.05$. Blue * indicates a significant difference compared to the sh-SAMHD1 + oe-NC group, with $p < 0.05$. (The data are presented as mean \pm standard deviation, and an independent sample t-test was used for statistical analysis. The experiment was repeated 3 times.)

their correlation. Initially, co-transfecting EC cells with plasmids overexpressing SAMHD1 and TRIM27, we observed a positive correlation between the protein levels of TRIM27 and SAMHD1, alongside enhanced PTEN Ub-k27 ubiquitination modification, indicating that SAMHD1 may promote PTEN Ub-k27 ubiquitination through upregulating TRIM27 expression (Fig. 6G-H). Furthermore, we validated cell proliferation using the CCK-8 method. The results indicate a significant impact on cell proliferation by si-TRIM27-2. Subsequently, we conducted ubiquitination detection on TRIM27-silenced cells, with si-TRIM27-2 showing the most effective silencing effect. Hence, si-TRIM27-2 was chosen for subsequent experiments (Fig. 6I-J). By inhibiting ubiquitin-proteasome degradation with MG132, the ubiquitination detection results showed that silencing TRIM27 suppressed the Ub-K27 ubiquitination of PTEN, indicating

that SAMHD1 regulates PTEN Ub-K27 ubiquitination through TRIM27 (Fig. 6K). Subsequently, ubiquitinated and non-ubiquitinated PTEN were immunopurified from cells (Fig. 6L). Following incubation of cells with different concentrations of purified ubiquitinated and non-ubiquitinated PTEN for 24 h, phosphatase activity was assessed by ELISA to measure PIP2 accumulation. The results revealed a significant decrease in phosphatase activity of ubiquitinated PTEN, leading to a further reduction in PIP2 levels due to increased ubiquitination of PTEN (Fig. 6M). Building on the earlier findings (Fig. 6L), overexpression of SAMHD1 was shown to elevate ubiquitinated PTEN protein levels. Combining these results with those in Fig. 6M, we conclude that SAMHD1 modulates PTEN phosphatase activity through ubiquitination, thereby regulating the PI3K/AKT signaling pathway to

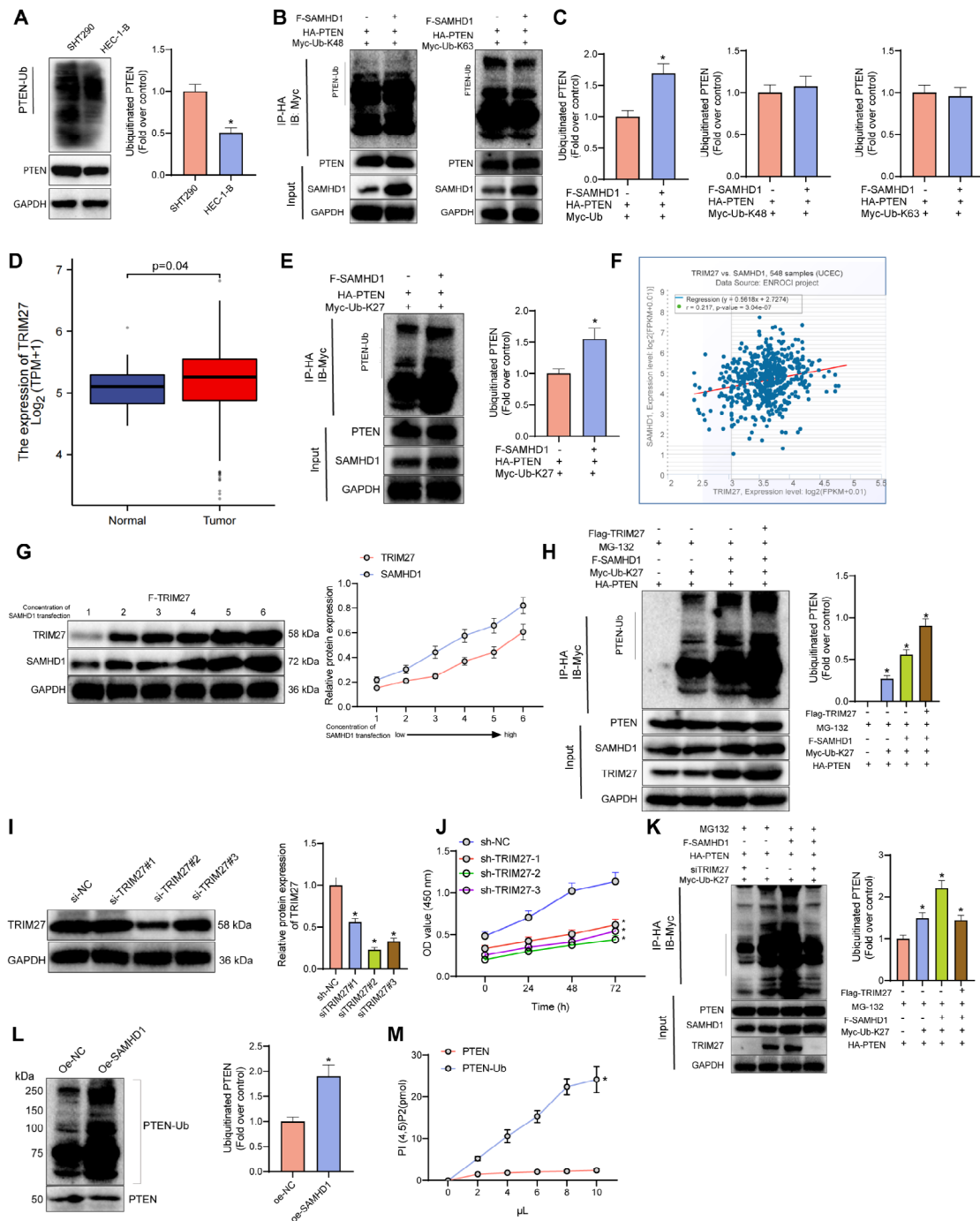


Fig. 6 Impact of SAMHD1 on the PTEN phosphatase activity mediated by TRIM27-induced PTEN ubiquitination modification *Note* (A) Western blot detection of the ubiquitination levels of PTEN in the normal immortalized endometrial stromal cell line SHT290 and the endometrial cancer cell line HEC-1-B; (B) Western blot detection of the effect of SAMHD1 on PTEN ubiquitination; (C) Western blot detection of the effect of SAMHD1 on PTEN Ub-k48 and Ub-k63 ubiquitination; (D) Expression of TRIM27 in TCGA-UCEC; (E) Western blot detection of the regulation of PTEN Ub-k27 ubiquitination by SAMHD1; (F) The correlation between the expression of SAMHD1 and TRIM27 in TCGA-UCEC is depicted by plotting a set of data points and drawing a red trend line to represent the relationship trend between the variables; (G) Western blot detection of the effect of SAMHD1 on TRIM27 expression; (H) Western blot detection of the effect of SAMHD1 on PTEN Ub-k27 ubiquitination mediated by TRIM27; (I) Western blot detection of the efficiency of siTRIM27; (J) CCK8 to detect the cell viability after silencing of TRIM27; (K) Western blot detection of the effect of silencing TRIM27 on SAMHD1-mediated PTEN Ub-k27 ubiquitination; (L) Immunoprecipitation to obtain ubiquitinated PTEN and non-ubiquitinated PTEN; (M) ELISA to detect the effect of SAMHD1 on PTEN phosphatase activity (the data are presented as mean ± standard deviation, and the experiment was repeated three times). Data comparison between the two groups was analyzed using independent samples t-test, while multiple groups were analyzed using one-way analysis of variance. Different time points were analyzed using two-way analysis of variance, with * indicating comparison with the first group in each result, and $p < 0.05$ signifying statistical significance

promote proliferation, migration, and invasion of EC cells.

Intratumoral transplantation experiments confirmed that knocking out SAMHD1 inhibits tumor progression by suppressing the PTEN/PI3K/AKT pathway

To investigate whether the SAMHD1-mediated upregulation of TRIM27 promotes PTEN ubiquitination at K27 and facilitates the progression of EC, we established a xenograft mouse model of EC. We knocked out SAMHD1 in the human EC cell line HEC-1-B and transplanted it subcutaneously into nude mice. The nude mice were divided into the following groups: (1) sh-NC; (2) sh-SAMHD1; (3) sh-NC+740 Y-P (PI3K activator)/SC-79 (AKT activator); (4) sh-SAMHD1+740 Y-P/SC-79.

Within 20 days after tumor transplantation, the tumor growth curve results showed (Fig. 7A) that compared to the NC group, the tumor growth was significantly inhibited in the sh-SAMHD1 group (*), while the tumor growth was promoted in the sh-SAMHD1+740 Y-P/SC-79 group compared to the sh-SAMHD1 group (#), suggesting that the activation of PI3K/AKT could promote tumor growth. After removing the tumors, they were photographed and weighed (Fig. 7B-C). Compared to the sh-NC group, the tumor size and weight were significantly reduced in the sh-SAMHD1 group, while they were significantly increased in the sh-SAMHD1+740 Y-P/SC-79 group compared to the sh-SAMHD1 group. The apoptotic status of tumor cells was analyzed by

TUNEL assay, which showed that compared to the sh-NC group, tumor cell apoptosis was significantly increased in the sh-SAMHD1 group, while it was significantly decreased in the sh-SAMHD1+740 Y-P/SC-79 group compared to the sh-SAMHD1 group (Fig. 7D). Immunohistochemistry staining for Ki67 showed that compared to the NC group, the proliferation rate of tumor cells was significantly reduced in the sh-SAMHD1 group, while it was significantly increased in the sh-SAMHD1+740 Y-P/SC-79 group compared to the sh-SAMHD1 group (Fig. 7E). These findings indicate that the knockdown of SAMHD1 can significantly inhibit tumor growth in vivo, but the tumor growth inhibitory effect caused by SAMHD1 can be reversed by providing a PI3K and AKT agonist (740 Y-P/SC-79).

The Western blot results of tumor tissue (Fig. 7F-G) showed that compared to the NC group, the sh-SAMHD1 group had significantly decreased TRIM27, significantly reduced PTEN ubiquitination, and suppressed phosphorylation of the PI3K/AKT pathway. However, when PI3K/AKT activators were administered in the context of sh-SAMHD1, they did not significantly impact the expression levels of TRIM27 and PTEN but instead promoted the activation of the PI3K/AKT pathway. The in vivo tumor transplantation experiment further confirmed that knocking out SAMHD1 suppressed tumor progression, primarily by downregulating TRIM27. Moreover, the inhibition of PI3K/AKT activity was linked to the

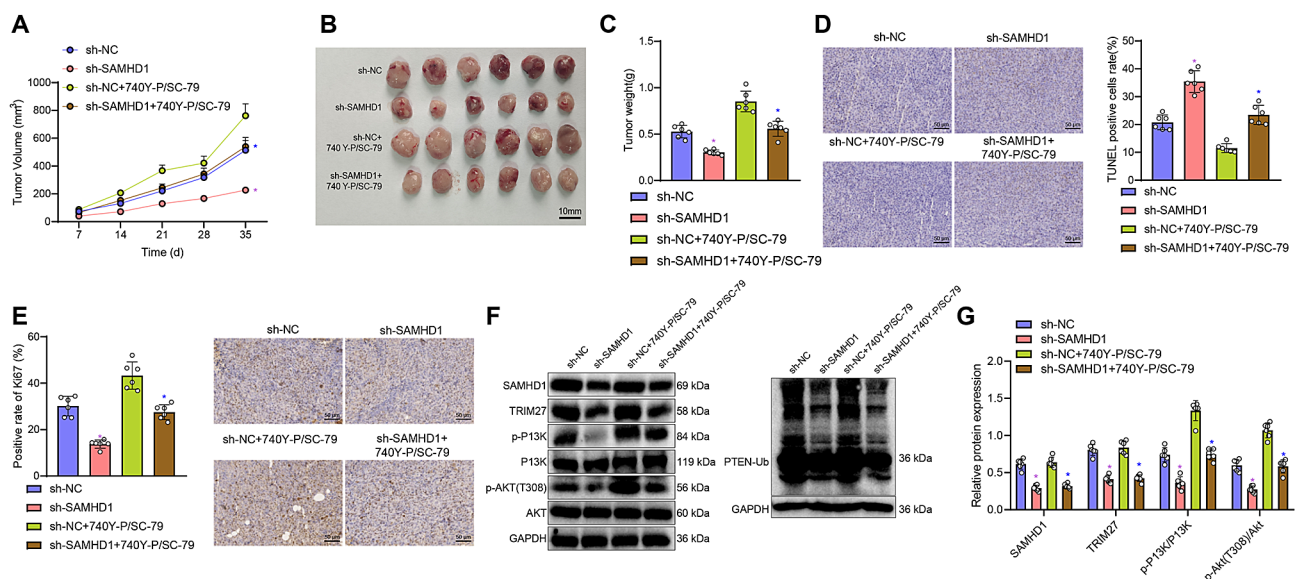


Fig. 7 SAMHD1 knockout inhibits tumor progression by suppressing the PTEN/PI3K/AKT pathway *Note* (A) Tumor growth curve of HEC-1-B tumor-bearing mice; (B) Tumor size; (C) Tumor weight statistics; (D) TUNEL staining for apoptosis level in tumor tissue (scale bar = 50 μ m); (E) Ki67 staining for proliferation level in tumor tissue (scale bar = 50 μ m); (F-G) Western blot for expression of tumor-related proteins in tumor tissue. $N=6$. For multiple group data, one-way analysis of variance was conducted, with pairwise comparisons between groups analyzed using Tukey's test. Tumor volume data at different time points were analyzed using repeated measures analysis of variance. (* in purple indicates comparison with shNC, $p < 0.05$; * in blue indicates comparison with shSAMHD1, $p < 0.05$)

reduced ubiquitination of PTEN, which subsequently enhanced PTEN phosphatase activity.

Discussion

Previous studies have demonstrated that SAMHD1 is highly expressed in various cancers, including endometrial cancer (EC), where it is associated with the malignant phenotype of EC cells [35]. Our findings align with these studies, further supporting the significant role of SAMHD1 in cancer progression [10]. However, it is crucial to recognize that the specific mechanisms and regulatory networks of SAMHD1 in EC may differ from those in other cancers, warranting further investigation [10]. SAMHD1 likely engages in complex interactions with various proteins and signaling pathways, which might be unique to EC [36].

With the growing application of big data in biomedical research, databases such as TCGA and GEO have become indispensable tools for comprehensive cancer gene expression analysis [37]. Compared to traditional studies that rely on single datasets or small-scale laboratory samples, multi-database analysis offers larger sample sizes and enhances the reliability and generalizability of the results [38]. In our study, we effectively utilized these databases to identify a strong association between SAMHD1 and EC, showcasing the great potential of data mining in uncovering novel insights into cancer biology.

Our research also highlights the relationship between SAMHD1 and TRIM27-mediated PTEN ubiquitination, a connection that has been rarely explored in the literature [10]. Previous research has indicated that TRIM27 is involved in promoting PI3K/AKT signaling by interacting with phosphatases and reducing the activity of PTEN [15, 18]. Our findings expand on this knowledge by demonstrating that SAMHD1 positively regulates TRIM27-mediated PTEN ubiquitination, further influencing the downstream PI3K/AKT signaling pathway. This discovery provides new insights into the ubiquitination regulation mechanism of SAMHD1.

Interestingly, our study revealed that SAMHD1 primarily modulates the phosphatase activity of PTEN through Ub-k27 ubiquitination, while it does not affect Ub-k48 and Ub-k63 ubiquitination. This suggests a specific regulatory mechanism by which SAMHD1 modulates PTEN function, highlighting the potential for targeted therapeutic strategies in EC. Additionally, while we hypothesize that there might be an interaction between SAMHD1 and TRIM27, further evidence is required to confirm this.

The activation of the PI3K/AKT signaling pathway is closely associated with the progression and worsening of various cancers, including EC [39]. Our study contributes to this understanding by showing that SAMHD1 overexpression can indirectly activate this pathway, although

there are some discrepancies with previous research findings [40, 41]. These discrepancies might be due to differences in cancer cell types or other unidentified factors. Nonetheless, our results indicate that silencing SAMHD1 reduces the expression of PI3K and AKT signaling components, suggesting that modulating SAMHD1 expression could be a viable strategy for inhibiting EC cell proliferation, migration, and invasion.

In conclusion, our research underscores the critical role of the PI3K/AKT signaling pathway in EC development and progression. By elucidating the regulatory relationship between SAMHD1, TRIM27-mediated PTEN ubiquitination, and the PI3K/AKT pathway, we propose novel targeted strategies for EC treatment that could improve therapeutic efficacy and enhance patients' quality of life. Additionally, our study offers new markers for early diagnosis and prognosis assessment, potentially paving the way for innovative therapies for EC.

The activation of the PI3K/AKT signaling pathway is closely associated with the progression and deterioration of various cancers [39]. Our study revealed that overexpression of SAMHD1 can indirectly activate this signaling pathway, showing some discrepancies from previous research findings [40, 41]. These discrepancies may arise from the type of cancer, cell specificity, or other as yet unidentified factors. Furthermore, silencing SAMHD1 led to a reduction in the expression of the PI3K and AKT signaling pathways. Activation of PI3K/AKT effectively inhibits proliferation, migration, and invasion of EC cells. We hypothesize that modulating the overexpression of SAMHD1 by silencing the PI3K/AKT signaling pathway may be beneficial in suppressing the proliferation, migration, and invasion of EC cells, but this requires further validation. In conclusion, the activation of the PI3K/AKT signaling pathway holds significant importance in the occurrence and development of EC. Through this research, we discovered that SAMHD1 regulates the relationship between TRIM27-mediated PTEN ubiquitination modification and EC, providing novel targeted strategies for EC treatment to improve therapeutic efficacy and patients' quality of life, with significant scientific and clinical implications. Additionally, an in-depth exploration of the key molecular regulatory networks of EC not only offers new markers for early diagnosis and prognosis assessment of EC but also potentially paves the way for novel targeted therapies for EC.

We also validated the impact of SAMHD1 on EC using a xenograft mouse model. In comparison to studies solely based on cell culture experiments, animal models can provide more realistic evidence of biological effects (Fig. 8). Of course, no model can completely replicate the human environment, yet validating the function of genes *in vivo* is invaluable.

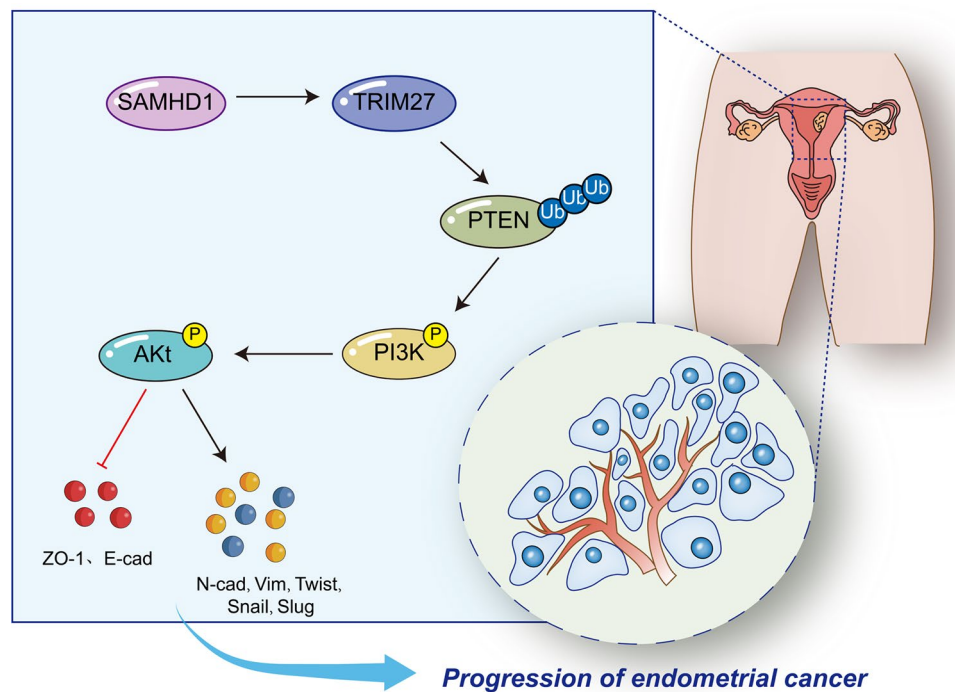


Fig. 8 SAMHD1 regulates the molecular mechanism of PTEN ubiquitination mediated by TRIM27, affecting the occurrence and development of endometrial cancer

Conclusion

Lastly, despite providing numerous new insights and data in the field of EC, our study has some limitations, such as sample size and experimental conditions. In the future, investigating whether overexpression of SAMHD1 in normal endometrial stromal cell lines poses a risk for EC could be explored. Furthermore, validating whether SAMHD1 has a broad-spectrum therapeutic effect on other types of EC cells is necessary. Comprehensive sample collection and more in-depth mechanistic studies will further reveal the detailed role of SAMHD1 in EC.

Materials and methods

Bioinformatics analysis

The datasets GSE17025 and GSE63678 were downloaded from the Gene Expression Omnibus (GEO) database (<https://www.ncbi.nlm.nih.gov/gds>). GSE17025 contained 12 atrophic endometrial tissues and 91 samples of EC tissues. GSE63678 included 5 samples of normal endometrial tissues and 7 samples of EC tissues. The expression difference of SAMHD1 between the control group and the EC group was compared using the Welch t-test. The expression and correlation of SAMHD1 and TRIM27 in EC from The Cancer Genome Atlas (TCGA) were analyzed using the ENCORI database (<https://starbase.sysu.edu.cn/index.php>).

Cell culture

The human EC cell lines (KLE, HEC-1-B, RL95-2, Ishikawa) and human immortalized endometrial stromal cell line SHT290 were obtained from ATCC (USA). The HEC-1-B cells were cultured in MEM medium (Gibco, USA) supplemented with 10% serum. Ishikawa, RL95-2, and KLE cells were cultured in DMEM/F-12 medium (Gibco, USA) as referenced [42, 43]. SHT290 was cultured in phenol red-free DMEM (Gibco) containing 2% charcoal-stripped FBS and 1x GlutaMax (Gibco) as cited [44]. All the cell culture media were supplemented with 10 µg/mL streptomycin and 100 U/mL penicillin (Gibco, USA). The cells were incubated at 37°C in a 5% CO₂ incubator (Thermo, USA) with regular media change every 2–3 days until cell confluence reached about 80%. The cells were dissociated using trypsin, centrifuged at 300 g, and then diluted in an antibiotic-free medium to a specific concentration before seeding at a quantity of 1×10^5 cells per well in a 6-well plate. After routine incubation for 24 h and reaching approximately 75% confluency, the cells were transfected following the instructions of Lipofectamine 2000 (Invitrogen). Specifically, 20 pmol of siRNA was diluted in 50 µL Opti-MEM serum-free medium and mixed gently. Lipofectamine 2000 was pre-mixed before adding 1 µL to the siRNA solution in 50 µL Opti-MEM medium, and incubated at room temperature for 5 minutes. The diluted DNA and Lipofectamine 2000 were mixed gently and left at room temperature for

20 min. 100 μ L of the transfection mixture was added to each well. The cells were then treated with 740 Y-P (PI3K activator) (20 μ M, Tocris Bioscience, Ellisville, MO, USA) and SC-79 (AKT phosphorylation activator) (4 μ g/mL, Sigma, USA) as indicated [45, 46], for 24 h before assessing gene expression following 24 h of incubation at 37°C.

Cell transfection

Expressed plasmid vector (OE-NC), SAMHD1 (OE-SAMHD1/F-SAMHD1), PTEN (HA-PTEN), TRIM27 (F-TRIM27) [47], Ub(Myc-Ub) [48], Ub-k27(Myc-Ub-k27) [49], Ub-k48(Myc-Ub-k48) [50], Ub-k63(Myc-Ub-k63) [51]. These plasmids were purchased from Addgene. The genes were cloned into the pRK5-HA vector. The sh-NC plasmid for gene silencing was purchased from Sigma. shRNA was cloned into the PLKO.1 vector (sh-NC, Sigma). The target sequences for siRNA and shRNA can be found in Supplementary Table S1

The plasmid transfection and silencing groups were organized as follows: (1) oe-NC group: transfected with the oe-NC plasmid; (2) oe-SAMHD1 group: transfected with the OE-SAMHD1/F-SAMHD1 plasmid; (3) sh-NC group: transfected with the sh-NC plasmid; (4) sh-SAMHD1 group: transfected with the sh-SAMHD1 plasmid. Additionally, the following combined groups were created: (5) sh-NC+oe-NC group: simultaneous transfection of oe-NC and sh-NC plasmids; (6) sh-NC+oe-PTEN group: simultaneous transfection of sh-NC and oe-PTEN plasmids; (7) sh-SAMHD1+oe-NC group: simultaneous transfection of sh-SAMHD1 and oe-NC plasmids; (8) sh-SAMHD1+oe-PTEN group: simultaneous transfection of sh-SAMHD1 and oe-PTEN plasmids. After 48 h of transfection, a portion of the cells was taken to verify the efficiency of knockdown and overexpression at the protein and RNA levels [52].

qRT-PCR

Total RNA was extracted using TRIzol Reagent (15596026, Invitrogen, Car, Cal, USA). The RNA was reverse transcribed into cDNA using the Quantitative RT-PCR Thermo Script One-Step System (11731023, Invitrogen, Car, Cal, USA) according to the manufacturer's instructions. The cDNA was then subjected to qPCR analysis using the Fast SYBR Green PCR Kit (Applied Biosystems) on an ABI PRISM 7300 RT-PCR system (Applied Biosystems), with three replicates per well. GAPDH was used as an internal control, and the relative gene expression was analyzed using the $2^{-\Delta\Delta C_t}$ method. The qRT-PCR primer sequences are listed in Supplementary Table S2.

Western blot

Cultured cells from different groups were collected using the trypsin digestion method. The cells were lysed with

enhanced RIPA lysis buffer containing a protease inhibitor (89900, Invitrogen, Car, Cal, USA), and the protein concentration was determined using the BCA Protein Assay Kit (23235, Invitrogen, Car, Cal, USA). The proteins were separated by 10% SDS-PAGE gel electrophoresis, and then transferred to a PVDF membrane. Nonspecific binding was blocked by incubating with 5% BSA at room temperature for 2 h. The membrane was incubated with diluted primary antibodies overnight at 4°C. After washing the membrane, it was incubated with HRP-conjugated goat anti-rabbit secondary antibody at room temperature for 1 h. The membrane was then incubated with ECL working solution (35055, Invitrogen, Car, Cal, USA) at room temperature for 1 min, excess ECL reagent was removed, and the membrane was exposed using the Bio-Rad gel imaging system. The intensity of protein bands in Western blot was analyzed using ImageLab analysis software, with GAPDH as the internal control. Each experiment was repeated three times. Antibody sources are shown in Supplementary Table S3.

Immunoprecipitation assay

The cells were lysed in BC100 lysis buffer (20 mM Tris-HCl pH 7.3, 100 mM NaCl, 10% glycerol, 0.2 mM EDTA, 0.2% Triton X-100, and protease inhibitors) to investigate the interaction between SAMHD1 and PTEN proteins. A portion of the extract was then saved as the input, while the remaining extract was incubated with SAMHD1 antibody (1:50, ab264335, Abcam, USA) or PTEN antibody (1:30, ab267787, Abcam, USA) at 4°C for 1 h. A/G Plus-Agarose beads (Santa Cruz, Biotechnology) were added and incubated overnight at 4°C. After extensive washing, the bound proteins were dissociated with the SDS sample buffer and subjected to Western blot analysis for protein detection.

CCK-8 method

The sorted cell populations were seeded into a 96-well culture plate at 1×10^3 cells/well density in 100 μ L of culture medium containing 10% FBS. The cells were then cultured for 0, 24, 48, and 72 h, and the cell count was determined using a cell counting kit (CCK8 method, Dojindo) according to the manufacturer's instructions. Afterward, 10 μ L of CCK8 solution was added to each well and incubated for 1 h, and the absorbance was measured at 450 nm using a SpectraMax 190 microplate reader (Bio-Rad Model 680).

The scratch assay detects the migration ability of EC cells

Horizontal lines were drawn evenly spaced at 0.5–1 cm intervals on the bottom of each well plate using a ruler and a marker pen. At least five lines were drawn per well. Approximately 5×10^5 cells were added per well into each 6-well plate. The cells were cultured overnight

in a growth medium containing 10% fetal bovine serum. Scratches were made vertically along the drawn lines using a sterile 10 μ L pipette tip. The distance of the scratches was measured under a microscope at 0 h and 24 h of incubation. Images of the scratches were captured using an inverted microscope, and the migration of cells in different groups was observed.

Transwell

The Matrigel provided by BD Company was used to coat the upper surface of the Transwell insert membrane and allowed to gel at 37 °C for 30 min. The basement membrane was hydrated before use. Cells were cultured in a serum-free medium for 12 h, harvested and resuspended in a serum-free medium (1×10^5 /ml). 100 μ l of the cell suspension was added to the Transwell insert with a medium containing 10% fetal bovine serum in the lower chamber. After incubation at 37 °C for 24 h, cells not invading the surface of the Matrigel membrane were gently wiped off using a cotton swab. Cells were fixed with methanol and stained with 1% toluidine blue (Sigma). Stained cells were observed under an inverted microscope (Carl Zeiss, Germany), and 5 randomly selected areas were manually counted for analysis of cell invasion. Each experiment was repeated 3 times.

Construction of subcutaneous xenograft model in nude mice

Forty-eight healthy BALB/c nude mice, aged 6–8 weeks, were purchased from the Animal Experiment Center of Jiangsu University (China, Jiangsu). The mice were housed in individual cages in a specific pathogen-free (SPF) animal facility. The laboratory had a humidity level of 60%–65% and a temperature range of 22–25 °C. The mice had 12 h of light and dark cycle and had ad libitum access to food and water. After one week of adaptation, the mice were assessed for their health status before the start of the experiment. The Animal Ethics Committee of our institution approved the experimental procedures and animal usage protocols.

To investigate the effect of SAMHD1 on the *in vivo* growth of EC cells, stable overexpression of SAMHD1 (oe-SAMHD1) Ishikawa cells and stable knockdown of SAMHD1 (sh-SAMHD1) HEC-1-B cells, as well as their corresponding control groups (oe-NC and sh-NC), were subcutaneously implanted into the nude mice. The mice were randomly divided into four groups: (1) oe-NC, (2) oe-SAMHD1, (3) sh-NC, (4) sh-SAMHD1. Each group consisted of 6 mice. The mice were injected with 1×10^6 cells/100 μ L HEC-1-B cells subcutaneously, and the tumor volume was measured weekly. After four weeks, the mice were euthanized, and the tumors were photographed.

After knocking out SAMHD1 in the human EC cell line HEC-1-B, a subcutaneous transplantation experiment was performed in nude mice to investigate the effect of the PI3K activator and AKT activator on tumor growth. The nude mice were randomly divided into four groups: (1) sh-NC; (2) sh-SAMHD1; (3) sh-NC+740 Y-P (PI3K activator)/SC-79 (AKT activator); (4) sh-SAMHD1+740 Y-P/SC-79. Each group consisted of 6 mice. The mice were injected with 1×10^6 cells/100 μ L HEC-1-B cells subcutaneously. The tumor volume was measured every 5 days, and the tumor weight was calculated after 3 weeks of transplantation.

H&E staining

The tissue samples were fixed in 10% formalin (pH 7.4), embedded in paraffin, and then sectioned. The sections were dewaxed twice for 10 min each, followed by gradient ethanol dehydration, 2-minute distilled water wash, 7-minute hematoxylin staining, 10-minute tap water rinse, another distilled water wash, 5-second 95% ethanol, and 1-minute eosin staining. The sections were then hydrated in gradient ethanol twice for 2 min each, cleared in xylene twice for 5 min each, air-dried in a fume hood, and finally examined under an optical microscope for morphological changes in the nude mouse tumor tissues. Each experiment was repeated three times.

Detection of Ki67 protein

The organization samples were fixed in 10% formalin (pH 7.4) and embedded in paraffin. After sectioning, they were placed on glass slides and stained with Thermo Fisher Scientific's monoclonal antibody (PA5-114437, 1:200) targeting Ki67. Subsequently, counterstaining and visualization were performed using standard methods. Observations were made using an inverted optical microscope, with each experiment repeated three times [53].

TUNEL staining

According to the instruction manual of Roche's TUNEL assay kit, TUNEL staining was performed to detect cell apoptosis in nude mouse tumor tissue. The specific steps are as follows: the tissue sections were soaked in 0.3% H_2O_2 , then incubated with TUNEL-labeling buffer at 37 °C for 120 min, followed by treatment with an avidin-biotin-peroxidase complex solution at 37 °C for 30 min. The sections were washed with PBS, then immersed in DAB solution for 10 min. The sections were observed under a fluorescence microscope, and cell counting was performed to calculate the proportion of TUNEL-positive cells (number of TUNEL-positive cells/total number of cells).

ELISA assay

The ELISA kit from Echelon Biosciences was used to perform experiments according to the manufacturer's instructions. First, the standard curve was prepared by diluting PTEN and PTEN-Ub to the same concentration. Then, a series of concentrations of PTEN and PTEN-Ub, along with the PIP2 detector and HRP conjugate, were gradually added. The mixture was incubated for 1 h in a culture dish and the absorbance was measured to quantify the amount of PIP2 using a colorimetric assay. Immunopurified ubiquitinated PTEN and non-ubiquitinated PTEN were collected from various cells. The amount of PIP2 generated from P3 under PTEN phosphatase activity was detected using ELISA, and the concentration was calculated using absorbance values and a standard curve.

Statistical analysis

The data statistical analysis used in this study was performed using SPSS 21.0 (IBM, USA) software. Continuous variables were presented as mean \pm standard deviation. Normality and homogeneity of variances tests were conducted first. If the data followed a normal distribution and had homogeneity of variances, a non-paired t-test was used for between-group comparisons, one-way analysis of variance was used for multiple group comparisons, and repeated-measures analysis of variance was used for tumor data at different time points, with post-hoc analysis performed using Tukey's method. A P value less than 0.05 was considered statistically significant.

Abbreviations

EC Endometrial cancer

Supplementary Information

The online version contains supplementary material available at <https://doi.org/10.1186/s13062-024-00525-7>.

Supplementary Material 1

Supplementary Material 2

Acknowledgements

None.

Author contributions

Ping Qiang and Ying Chen conceived and designed the study. Yang Shao and Qicheng Deng conducted the experiments and performed data analysis. Songyuan Xu contributed to bioinformatics analysis and data interpretation. Weipei Zhu supervised the project, provided critical revisions, and approved the final manuscript. All authors contributed to manuscript writing and approved the submitted version.

Funding

This study was funded by the project of Jiangsu Maternal and Child Health (F201843).

Data availability

Data will be made available on request.

Declarations

Ethical approval

The current study was approved by the Animal Ethics Committee of The First People's Hospital of Zhangjiagang City and performed according to the Guide for the Care and Use of Laboratory Animals by the US National Institutes of Health. The clinical experiments were approved by the Ethics Committee of The First People's Hospital of Zhangjiagang City, all the patients have been informed and signed informed consent before the experiments.

Consent for publication

Not applicable.

Competing interests

The authors declare no competing interests.

Received: 23 June 2024 / Accepted: 31 August 2024

Published online: 11 October 2024

References

- Gao S, Zhao T, Meng F, Luo Y, Li Y, Wang Y. Circular RNAs in endometrial carcinoma (review). *Oncol Rep.* 2022;48(6):212. <https://doi.org/10.3892/or.2022.8427>.
- Fan X, Fan YT, Zeng H, Dong XQ, Lu M, Zhang ZY. Role of ferroptosis in esophageal cancer and corresponding immunotherapy. *World J Gastrointest Oncol.* 2023;15(7):1105–18. <https://doi.org/10.4251/wjgo.v15.i7.1105>.
- Han P, Cao P, Hu S, et al. Esophageal microenvironment: from Precursor Microenvironment to Premetastatic Niche. *Cancer Manag Res.* 2020;12:5857–79. <https://doi.org/10.2147/CMAR.S258215>. Published 2020 Jul 16.
- Amant F, Moerman P, Neven P, Timmerman D, Van Limbergen E, Vergote I. Endometrial cancer. *Lancet.* 2005;366(9484):491–505. [https://doi.org/10.1016/S0140-6736\(05\)67063-8](https://doi.org/10.1016/S0140-6736(05)67063-8).
- Cong H, Yang X, Li Z et al. Salvage radiotherapy for locally recurrent cervical and endometrial carcinoma: clinical outcomes and toxicities. *BMC Cancer.* 2024;24(1):871. Published 2024 Jul 19. <https://doi.org/10.1186/s12885-024-12617-8>
- Berek JS, Matias-Guiu X, Creutzberg C et al. FIGO staging of endometrial cancer: 2023 [published correction appears in *Int J Gynaecol Obstet.* 2024;166(3):1374. doi: 10.1002/ijgo.15193]. *Int J Gynaecol Obstet.* 2023;162(2):383–394. <https://doi.org/10.1002/ijgo.14923>
- Hamilton CA, Pothuri B, Arend RC, et al. Endometrial cancer: a society of gynecologic oncology evidence-based review and recommendations. *Gynecol Oncol.* 2021;160(3):817–26. <https://doi.org/10.1016/j.ygyno.2020.12.021>.
- Zheng H, Zhang T, Xu Y, Lu X, Sang X. Autoimmune hepatitis after COVID-19 vaccination. *Front Immunol.* 2022;13:1035073. <https://doi.org/10.3389/fimmu.2022.1035073>. Published 2022 Nov 25.
- Yang J, Hu S, Bian Y, et al. Targeting cell death: pyroptosis, Ferroptosis, apoptosis and necroptosis in Osteoarthritis. *Front Cell Dev Biol.* 2022;9:789948. <https://doi.org/10.3389/fcell.2021.789948>. Published 2022 Jan 18.
- Coggins SA, Mahboubi B, Schinazi RF, Kim B. SAMHD1 functions and human diseases. *Viruses.* 2020;12(4):382. <https://doi.org/10.3390/v12040382>. Published 2020 Mar 31.
- Schumann T, Ramon SC, Schubert N, et al. Deficiency for SAMHD1 activates MDA5 in a cGAS/STING-dependent manner. *J Exp Med.* 2023;220(1):e20220829. <https://doi.org/10.1084/jem.20220829>.
- Helleday T, Rudd SG. Targeting the DNA damage response and repair in cancer through nucleotide metabolism. *Mol Oncol.* 2022;16(21):3792–810. <https://doi.org/10.1002/1878-0261.13227>.
- Maehigashi T, Lim C, Wade LR, et al. Biochemical functions and structure of *Caenorhabditis elegans* ZK177.8 protein: Aicardi-Goutières syndrome SAMHD1 dNTPase ortholog. *J Biol Chem.* 2023;299(9):105148. <https://doi.org/10.1016/j.jbc.2023.105148>.
- Morris ER, Caswell SJ, Kunzelmann S, et al. Crystal structures of SAMHD1 inhibitor complexes reveal the mechanism of water-mediated dNTP hydrolysis. *Nat Commun.* 2020;11(1):3165. <https://doi.org/10.1038/s41467-020-16983-2>. Published 2020 Jun 23.
- Yu C, Rao D, Wang T, Song J, Zhang L, Huang W. Emerging roles of TRIM27 in cancer and other human diseases. *Front Cell Dev Biol.* 2022;10:1004429. Published 2022 Sep 19. <https://doi.org/10.3389/fcell.2022.1004429>

16. Papa A, Pandolfi PP. The PTEN-PI3K Axis in Cancer. *Biomolecules*. 2019;9(4):153. <https://doi.org/10.3390/biom9040153>. Published 2019 Apr 17.
17. Yang Y, Zhu Y, Zhou S, et al. TRIM27 cooperates with STK38L to inhibit ULK1-mediated autophagy and promote tumorigenesis. *EMBO J*. 2022;41(14):e109777. <https://doi.org/10.15252/embj.2021109777>.
18. Lee JT, Shan J, Zhong J, et al. RFP-mediated ubiquitination of PTEN modulates its effect on AKT activation. *Cell Res*. 2013;23(4):552–64. <https://doi.org/10.1038/cr.2013.27>.
19. Xie P, Peng Z, Chen Y et al. Neddylation of PTEN regulates its nuclear import and promotes tumor development [published correction appears in *Cell Res*. 2021;31(3):374. doi: 10.1038/s41422-021-00470-4]. *Cell Res*. 2021;31(3):291–311. <https://doi.org/10.1038/s41422-020-00443-z>
20. Zhang F, Sun J, Tang X, et al. Stabilization of SAMHD1 by NONO is crucial for Ara-C resistance in AML. *Cell Death Dis*. 2022;13(7):590. <https://doi.org/10.1038/s41419-022-05023-0>. Published 2022 Jul 8.
21. Felip E, Gutiérrez-Chamorro L, Gómez M, et al. Modulation of DNA damage response by SAM and HD domain containing deoxynucleoside triphosphate triphosphohydrolase (SAMHD1) determines prognosis and treatment efficacy in different solid tumor types. *Cancers (Basel)*. 2022;14(3):641. <https://doi.org/10.3390/cancers14030641>. Published 2022 Jan 27.
22. An S, Vo TTL, Son T, et al. SAMHD1-induced endosomal FAK signaling promotes human renal clear cell carcinoma metastasis by activating Rac1-mediated lamellipodial protrusion. *Exp Mol Med*. 2023;55(4):779–93. <https://doi.org/10.1038/s12276-023-00961-x>.
23. Pastushenko I, Blanpain C. EMT Transition States during Tumor Progression and Metastasis. *Trends Cell Biol*. 2019;29(3):212–26. <https://doi.org/10.1016/j.tcb.2018.12.001>.
24. Zhou T, Luo M, Cai W, et al. Runt-related transcription factor 1 (RUNX1) promotes TGF- β -induced renal tubular epithelial-to-mesenchymal transition (EMT) and renal fibrosis through the PI3K subunit p110 δ . *EBioMedicine*. 2018;31:217–25. <https://doi.org/10.1016/j.ebiom.2018.04.023>.
25. Fan Y, Dong Z, Shi Y, Sun S, Wei B, Zhan L. NLR5 promotes cell migration and invasion by activating the PI3K/AKT signaling pathway in endometrial cancer. *J Int Med Res*. 2020;48(5):300060520925352. <https://doi.org/10.1177/0300060520925352>.
26. Cao X, He GZ. Knockdown of CLDN6 inhibits cell proliferation and migration via PI3K/AKT/mTOR signaling pathway in endometrial carcinoma cell line HEC-1-B. *Oncotargets Ther*. 2018;11:6351–60. <https://doi.org/10.2147/OTT.S174618>. Published 2018 Oct 1.
27. Kodigepalli KM, Bonifati S, Tirumuru N, Wu L. SAMHD1 modulates in vitro proliferation of acute myeloid leukemia-derived THP-1 cells through the PI3K-Akt-p27 axis. *Cell Cycle*. 2018;17(9):1124–37. <https://doi.org/10.1080/15384101.2018.1480218>.
28. Naderali E, Khaki AA, Rad JS, Ali-Hemmati A, Rahmati M, Charoudeh HN. Regulation and modulation of PTEN activity. *Mol Biol Rep*. 2018;45(6):2869–81. <https://doi.org/10.1007/s11033-018-4321-6>.
29. Fang S, Zhang D, Weng W, et al. CPSF7 regulates liver cancer growth and metastasis by facilitating WWP2-FL and targeting the WWP2/PTEN/AKT signaling pathway. *Biochim Biophys Acta Mol Cell Res*. 2020;1867(2):118624. <https://doi.org/10.1016/j.bbamcr.2019.118624>.
30. Shi YX, He YJ, Zhou Y, et al. LSD1 negatively regulates autophagy in myoblast cells by driving PTEN degradation. *Biochem Biophys Res Commun*. 2020;522(4):924–30. <https://doi.org/10.1016/j.bbrc.2019.11.182>.
31. Ma L, Yao N, Chen P, Zhuang Z. TRIM27 promotes the development of esophagus cancer via regulating PTEN/AKT signaling pathway. *Cancer Cell Int*. 2019;19:283. <https://doi.org/10.1186/s12935-019-0998-4>. Published 2019 Nov 8.
32. Heaton SM, Borg NA, Dixit VM. Ubiquitin in the activation and attenuation of innate antiviral immunity. *J Exp Med*. 2016;213(1):1–13. <https://doi.org/10.1084/jem.20151531>.
33. Hu H, Sun SC. Ubiquitin signaling in immune responses. *Cell Res*. 2016;26(4):457–83. <https://doi.org/10.1038/cr.2016.40>.
34. Ohtake F, Saeki Y, Ishido S, Kanno J, Tanaka K. The K48-K63 branched Ubiquitin Chain regulates NF- κ B signaling. *Mol Cell*. 2016;64(2):251–66. <https://doi.org/10.1016/j.molcel.2016.09.014>.
35. Crosbie EJ, Kitson SJ, McAlpine JN, Mukhopadhyay A, Powell ME, Singh N. Endometrial cancer. *Lancet*. 2022;399(10333):1412–28. [https://doi.org/10.1016/S0140-6736\(22\)00323-3](https://doi.org/10.1016/S0140-6736(22)00323-3).
36. Olsen RHJ, DiBerto JF, English JG, et al. TRUPATH, an open-source biosensor platform for interrogating the GPCR transducerome. *Nat Chem Biol*. 2020;16(8):841–9. <https://doi.org/10.1038/s41589-020-0535-8>.
37. Gong C, Fan Y, Zhou X, Lai S, Wang L, Liu J. Comprehensive Analysis of expression and Prognostic Value of GATAs in Lung Cancer. *J Cancer*. 2021;12(13):3862–76. <https://doi.org/10.7150/jca.52623>. Published 2021 May 5.
38. Xu L, Shao F, Luo T, Li Q, Tan D, Tan Y. Pan-cancer Analysis identifies CHD5 as a potential biomarker for Glioma. *Int J Mol Sci*. 2022;23(15):8489. <https://doi.org/10.3390/ijms23158489>. Published 2022 Jul 30.
39. Tian Z, Hao Y, Wang M, et al. Understanding the mechanism of twenty-five ingredient decoction for setting a fracture in the treatment of fractures based on network pharmacology. *Med (Baltim)*. 2023;102(5):e32864. <https://doi.org/10.1097/MD.00000000000032864>.
40. Patra KK, Bhattacharya A, Bhattacharya S. Allosteric Signal Transduction in HIV-1 restriction factor SAMHD1 proceeds via reciprocal handshake across monomers. *J Chem Inf Model*. 2017;57(10):2523–38. <https://doi.org/10.1021/acs.jcim.7b00279>.
41. Tollis S, Rizzotto A, Pham NT, et al. Chemical interrogation of nuclear size identifies compounds with Cancer Cell Line-Specific effects on Migration and Invasion. *ACS Chem Biol*. 2022;17(3):680–700. <https://doi.org/10.1021/acscchembio.2c00004>.
42. Zhu Y, Klausen C, Zhou J, et al. Novel dihydroartemisinin dimer containing nitrogen atoms inhibits growth of endometrial cancer cells and may correlate with increasing intracellular peroxynitrite. *Sci Rep*. 2019;9(1):15528. <https://doi.org/10.1038/s41598-019-52108-6>. Published 2019 Oct 29.
43. Zhou X, Duan J, Zhou W, Zhang A, Chen Q. Upregulated α -actinin-1 impairs endometrial epithelial cell adhesion by downregulating NEBL in recurrent implantation failure. *iScience*. 2024;27(3):109046. <https://doi.org/10.1016/j.isci.2024.109046>. Published 2024 Jan 26.
44. Hall JV, Schell M, Dessus-Babus S, et al. The multifaceted role of oestrogen in enhancing Chlamydia trachomatis infection in polarized human endometrial epithelial cells. *Cell Microbiol*. 2011;13(8):1183–99. <https://doi.org/10.1111/j.1462-5822.2011.01608.x>.
45. An G, Liang S, Sheng C, Liu Y, Yao W. Upregulation of microRNA-205 suppresses vascular endothelial growth factor expression-mediated PI3K/Akt signaling transduction in human keloid fibroblasts [retracted in: *Exp Biol Med (Maywood)*. 2023;248(23):2493. doi: 10.1177/15353702221144939]. *Exp Biol Med (Maywood)*. 2017;242(3):275–285. <https://doi.org/10.1177/1535370216669839>
46. Yang W, Yang Y, Xia L, et al. MiR-221 promotes Capan-2 pancreatic ductal adenocarcinoma cells proliferation by targeting PTEN-Akt. *Cell Physiol Biochem*. 2016;38(6):2366–74. <https://doi.org/10.1159/000445589>.
47. Nagahara H, Vocero-Akbani AM, Snyder EL, et al. Transduction of full-length TAT fusion proteins into mammalian cells: TAT-p27Kip1 induces cell migration. *Nat Med*. 1998;4(12):1449–52. <https://doi.org/10.1038/4042>.
48. Dantuma NP, Groothuis TA, Salomons FA, Neeffjes J. A dynamic ubiquitin equilibrium couples proteasomal activity to chromatin remodeling. *J Cell Biol*. 2006;173(1):19–26. <https://doi.org/10.1083/jcb.200510071>.
49. Terrell J, Shih S, Dunn R, Hicke L. A function for monoubiquitination in the internalization of a G protein-coupled receptor. *Mol Cell*. 1998;1(2):193–202. [https://doi.org/10.1016/s1097-2765\(00\)80020-9](https://doi.org/10.1016/s1097-2765(00)80020-9).
50. Lim KL, Chew KC, Tan JM, et al. Parkin mediates nonclassical, proteasomal-independent ubiquitination of synphilin-1: implications for Lewy body formation. *J Neurosci*. 2005;25(8):2002–9. <https://doi.org/10.1523/JNEUROSCI.4474-04.2005>.
51. Raasi S, Pickart CM. Ubiquitin chain synthesis. *Methods Mol Biol*. 2005;301:47–55. <https://doi.org/10.1385/1-59259-895-1-047>.
52. Wang Z, Ma XF, Wan CC, Zhang L, Wang JB, Zhongguo Shi. *Yan Xue Ye Xue Za Zhi*. 2022;30(5):1318–23. <https://doi.org/10.19746/j.cnki.issn.1009-2137.2022.05.003>.
53. Cheng R, Chen Y, Zhou H, Wang B, Du Q, Chen Y. B7-H3 expression and its correlation with clinicopathologic features, angiogenesis, and prognosis in intrahepatic cholangiocarcinoma. *APMIS*. 2018;126(5):396–402. <https://doi.org/10.1111/apm.12837>.

Publisher's note

Springer Nature remains neutral with regard to jurisdictional claims in published maps and institutional affiliations.